A New Ocean Color Algorithm: Simultaneous Retrieval of Aerosol Optical Properties and Chlorophyll Concentrations

Knut Stamnes and Wei Li
Stevens Institute of Technology
Hoboken, New Jersey 07030, USA

Banghua Yan
Decision Systems Technologies Inc.,
Rockville, MD 20850, USA

Andrew Barnard* **and Scott Pegau**
Oregon State University
Corvallis, OR 97331, USA

Jakob J. Stamnes
University of Bergen
N-5005, Bergen, Norway

*Present affiliation: Bigelow Laboratory for Ocean Science, 180 McKown Point Road, West Boothbay Harbor, ME 04575, USA

Outline of Talk

- Brief Introduction to Radiative Transfer in the Atmosphere-Ocean System
- Brief Review of the SeaWiFS Algorithm
- Description of the New Algorithm
- Algorithm Evaluation
- Summary and Conclusions

Light and Life Laboratory STEVENS Institute of Technology

Physical Overview of the Transfer of Solar Radiation in the Atmosphere - Ocean System

Light propagation in the atmosphere-ocean system depends on:

- Atmospheric optical properties including:

=> Absorption by molecules (H_2O, O_3, CO_2, and others)
=> Scattering by atmospheric molecules (Rayleigh scattering)
=> Scattering and absorption by aerosols

- Oceanic optical properties including:

=> Absorption by pure water
=> Scattering by density fluctuations (Rayleigh scattering)
=> Absorption by yellow substance or colored dissolved organic matter (CDOM)
=> Scattering and absorption by suspended particles
=> Scattering and absorption by air bubbles in the water column

Light propagation also depends on:

- Fresnel reflection and transmission through the atmosphere-ocean interface
- Scattering by surface roughness (foam, white caps)

In addition:

- sources of light due to fluorescence and Raman scattering may (depending on wavelength) contribute to the light field in the ocean.

Simulation of the solar signal in the atmosphere-ocean system

Physical overview

- Scattering and absorption by aerosol layer
- Scattering and absorption by algae cells
- Scattering and absorption by suspended matter
- Absorption by yellow matter

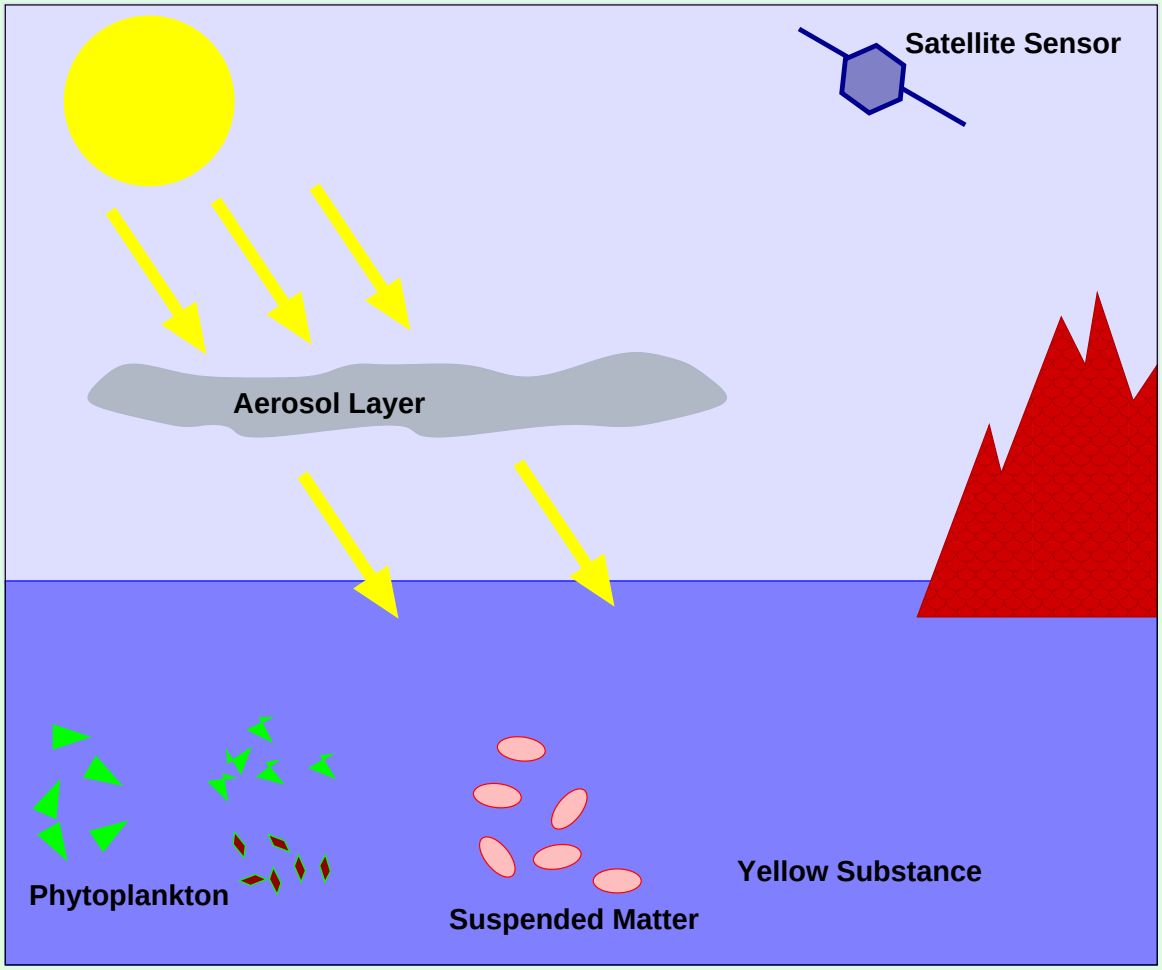

Figure 1: Illustration of Light Propagation In the Atmosphere-Ocean System

Radiative Transfer Modeling

We consider a vertically stratified medium for which the transfer of diffuse radiation is described by the equation ($I(\tau, u, \phi)$ = radiance; $u = \cos\theta$; θ = polar angle; ϕ = azimuthal angle):

$$u\frac{dI(\tau,u,\phi)}{d\tau} = I(\tau,u,\phi) - S(\tau,u,\phi), \tag{1}$$

$$S(\tau,u,\phi) = \frac{a(\tau)}{4\pi}\int_0^{2\pi} d\phi' \int_{-1}^{1} du' p(\tau,u',\phi',u,\phi) I(\tau,u',\phi') + S^*(\tau,u,\phi). \tag{2}$$

For the coupled atmosphere-ocean system, the change in the refractive index across the interface must be accounted for. From elementary optics we know that:

- **The refraction across the interface is described by Snell's law**
- **The reflection and transmission are described by Fresnel's equations**
- **The downward radiation distributed over 2π steradians in the atmosphere will be restricted to an angular cone less then 2π after being refracted into the ocean (see Figure below).**

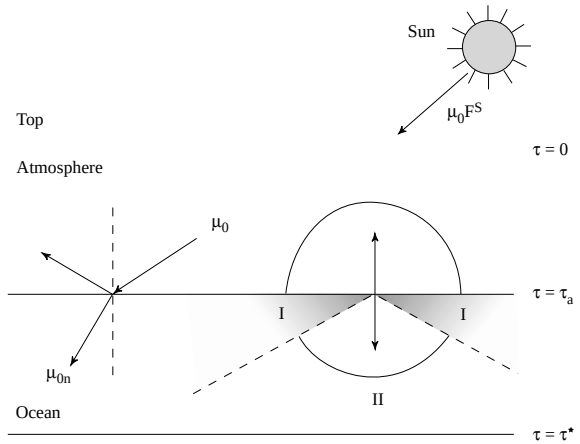

Figure 2: **Schematic illustration of two adjacent media with a flat interface: the atmosphere overlying a calm ocean.**

Definitions:

$$d\tau = [\alpha(z) + \sigma(z)]\, dz \quad \textbf{optical depth} \tag{3}$$

$$\alpha(z) = \textbf{absorption coefficient } [\mathrm{m}^{-1}] \tag{4}$$

$$\sigma(z) = \textbf{scattering coefficient } [\mathrm{m}^{-1}] \tag{5}$$

$$a(z) = \frac{\sigma(z)}{\alpha(z) + \sigma(z)} \quad \textbf{single scattering albedo} \tag{6}$$

$$\alpha(z) \equiv \sum_i \alpha^i(z) = \sum_i n^i\, \alpha_n^i\ ; \qquad \sigma(z) \equiv \sum_i \sigma^i(z) = \sum_i n_i\, \sigma_n^i \tag{7}$$

$$\alpha_n^i = \textbf{absorption cross section } [\mathrm{m}^2] \tag{8}$$

$$\sigma_n^i = \textbf{scattering cross section } [\mathrm{m}^2] \tag{9}$$

$$n_i = \textbf{concentration of } i^{\textbf{th}} \textbf{ species } [\mathrm{m}^{-3}] \tag{10}$$

Phase function (normalized angular scattering cross section):

$$p(\tau, \cos\Theta) = p(\tau, u', \phi'; u, \phi) = \frac{\sum_i\ \sigma^i(\tau, cos\Theta)}{\sum_i \int_{4\pi} d\ cos\Theta\ \sigma^i(\tau, cos\Theta)/4\pi} = \frac{\sum_i\ \sigma^i(\tau, cos\Theta)}{\sum_i\ \sigma^i(\tau)} = \frac{\sigma(\tau, cos\Theta)}{\sigma(\tau)} \tag{11}$$

$$\Theta = \textbf{scattering angle} \tag{12}$$

$$(\theta', \phi') = \textbf{polar and azimuthal angles } \textit{prior to } \textbf{scattering} \tag{13}$$

$$(\theta, \phi) = \textbf{polar and azimuthal angles } \textit{after } \textbf{scattering} \tag{14}$$

These angles are related through the cosine law of spherical geometry:

$$\cos\ \Theta = cos\ \theta'\ cos\theta + sin\ \theta'\ sin\ \theta\ cos(\phi' - \phi). \tag{15}$$

Factoring out Azimuthal Dependence - 1

- **Expand phase function in Legendre polynomials:**

$$p(\tau, \cos\ \Theta) \ = \ \sum_{l=0}^{2M-1} (2l+1)\chi_l(\tau)\ P_l(\cos\Theta) \tag{16}$$

where $P_l(\cos\Theta)$ is the Legendre polynomial and the expansion coefficients are given by:

$$\chi_l(\tau) \ = \ \frac{1}{2}\int_{-1}^{1} d\ \cos\Theta\ p(\tau, \cos\Theta)\ P_l(\cos\Theta) \tag{17}$$

- **Addition Theorem for Spherical Harmonics:**

$$P_l(cos\Theta) = P_l(u')P_l(u') + 2\sum_{m=1}^{l} \Lambda_m^l(u')\Lambda_l^m(u)\cos m(\phi' - \phi) \tag{18}$$

$$\Lambda_l^m(u) = \left[\frac{(l-m)!}{(l+m)!}\right]^{1/2} P_l^m(u) \tag{19}$$

- **The phase function now becomes:**

$$p(\tau, \cos\ \Theta) = p(u', \phi'; u, \phi) = \sum_{m=0}^{2M-1} (2 - \delta_{0m})\ p^m(u', u)\ cosm(\phi' - \phi)$$

where

$$p^m(u', u) = \sum_{l=m}^{2M-1} (2l+1)\ \chi_l\ \Lambda(u')\ \Lambda(u).$$

Factoring out Azimuthal Dependence - 2

- **Now expand radiance as:**

$$I(\tau, u, \phi) \;=\; \sum_{m=0}^{2N-1} \; I^m(\tau, u)\; \cos m(\phi_0 - \phi) \tag{20}$$

- **This leads to an equation for each Fourier component:**

$$u\frac{dI^m(\tau, u)}{d\tau} \;=\; I^m(\tau, u) - \frac{a(\tau)}{2}\int_{-1}^{1} p^m(\tau, u^{'}, u) I^m(\tau^{'}, u) du^{'} - X_0^m(\tau, u) e^{-\tau/\mu_0} \tag{21}$$

where

$$X_0^m(\tau, u) \;=\; \frac{a(\tau)}{2} F_0(2 - \delta_{0m}) p^m(\tau, \mu_0, u). \tag{22}$$

Discrete-Ordinate-Approximation

Because azimuthal components in Eq. (20) are uncoupled, we may focus on azimuthally-averaged radiance obtained by setting m = 0. We obtain a pair of coupled *Integro-differential* equations:

$$\mu\frac{dI^+(\tau,\mu)}{d\tau} = I^+(\tau,\mu) - \frac{a}{2}\int_0^1 d\mu' p(\mu',\mu)I^+(\tau,\mu') - \frac{a}{2}\int_0^1 d\mu' p(-\mu',\mu)I^-(\tau,\mu') - X_0^+ e^{-\tau/\mu_0} \quad (23)$$

$$-\mu\frac{dI^-(\tau,\mu)}{d\tau} = I^-(\tau,\mu) - \frac{a}{2}\int_0^1 d\mu' p(\mu',-\mu)I^+(\tau,\mu') - \frac{a}{2}\int_0^1 d\mu' p(-\mu',-\mu)I^-(\tau,\mu') - X_0^- e^{-\tau/\mu_0} \quad (24)$$

where $(\mu = |u|)$

$$p(\mu',\mu) = \sum_{l=0}^{2N-1}(2l+1)\chi_l P_l(\mu')P_l(\mu); \qquad X_0^{\pm} \equiv X_0(\pm\mu) = \frac{a}{4\pi}F_0 p(-\mu_0,\pm\mu)$$

Discrete-ordinate approximation:

- **Replace integrals in equations above by quadrature sums, thereby transforming:**
- ***pair of coupled integro-differential equations into a system of coupled differential equations:***

$$\mu_i\frac{dI^+(\tau,\mu_i)}{d\tau} = I^+(\tau,\mu_i) - \frac{a}{2}\sum_{j=1}^{N} w_j p(\mu_j,\mu_i)I^+(\tau,\mu_j) - \frac{a}{2}\sum_{j=1}^{N} w_j p(-\mu_j,\mu_i)I^-(\tau,\mu_j) - X_{0i}^+ \; e^{-\tau/\mu_0} \quad (25)$$

$$-\mu_i\frac{dI^-(\tau,\mu_i)}{d\tau} = I^-(\tau,\mu_i) - \frac{a}{2}\sum_{j=1}^{N} w_j p(\mu_j,-\mu_i)I^+(\tau,\mu_j) - \frac{a}{2}\sum_{j=1}^{N} w_j p(-\mu_j,-\mu_i)I^-(\tau,\mu_j) - X_{0i}^- \; e^{-\tau/\mu_0} \quad (26)$$

Comparison of DISORT Results with Monte Carlo Simulations

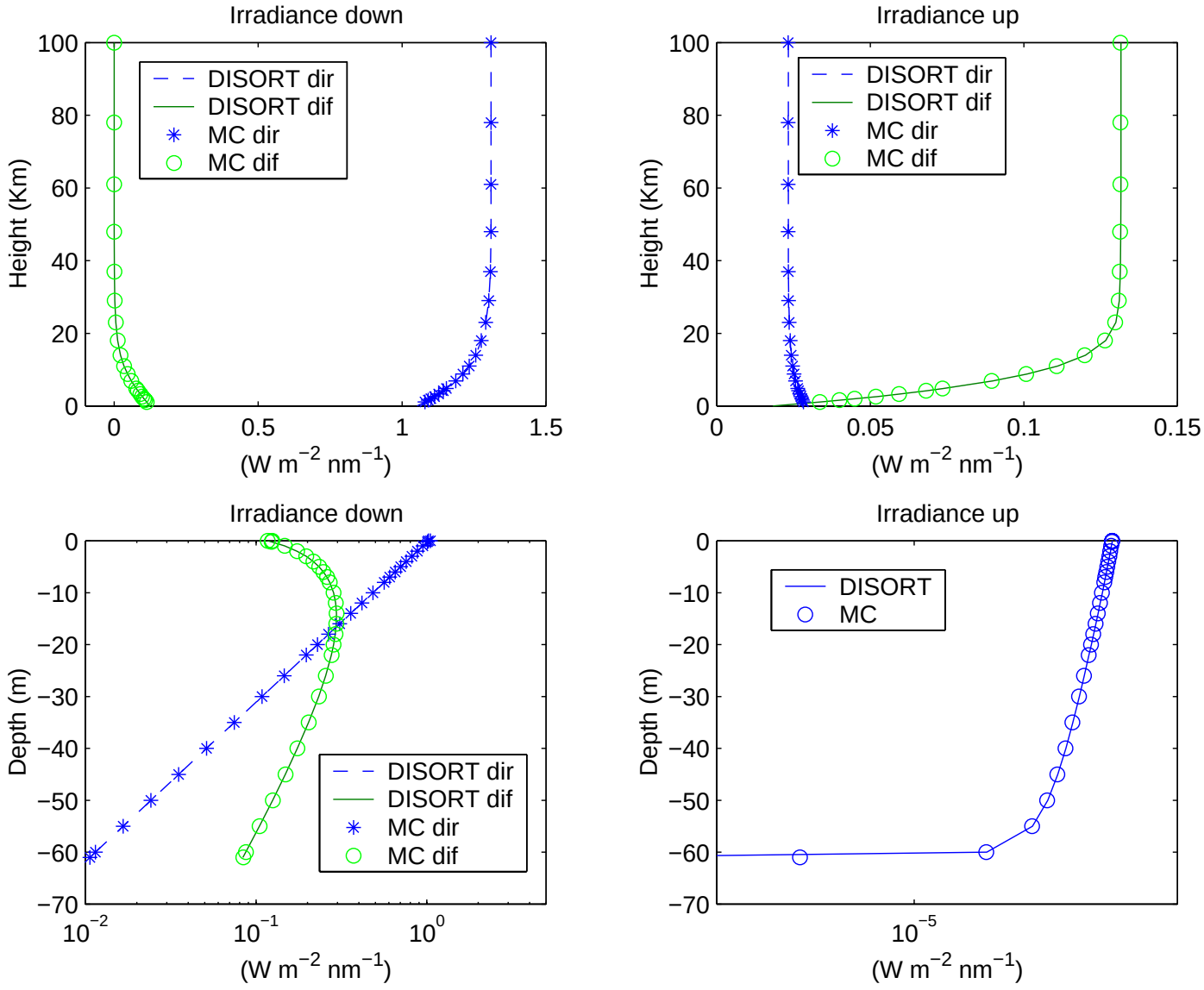

Figure 3: **Comparison of DISORT and Monte Carlo Results for the Coupled Atmopshere Ocean System. The Monte Carlo Computations are due to K. I. Gjerstad, University of Bergen (Gjerstad, 2001).**

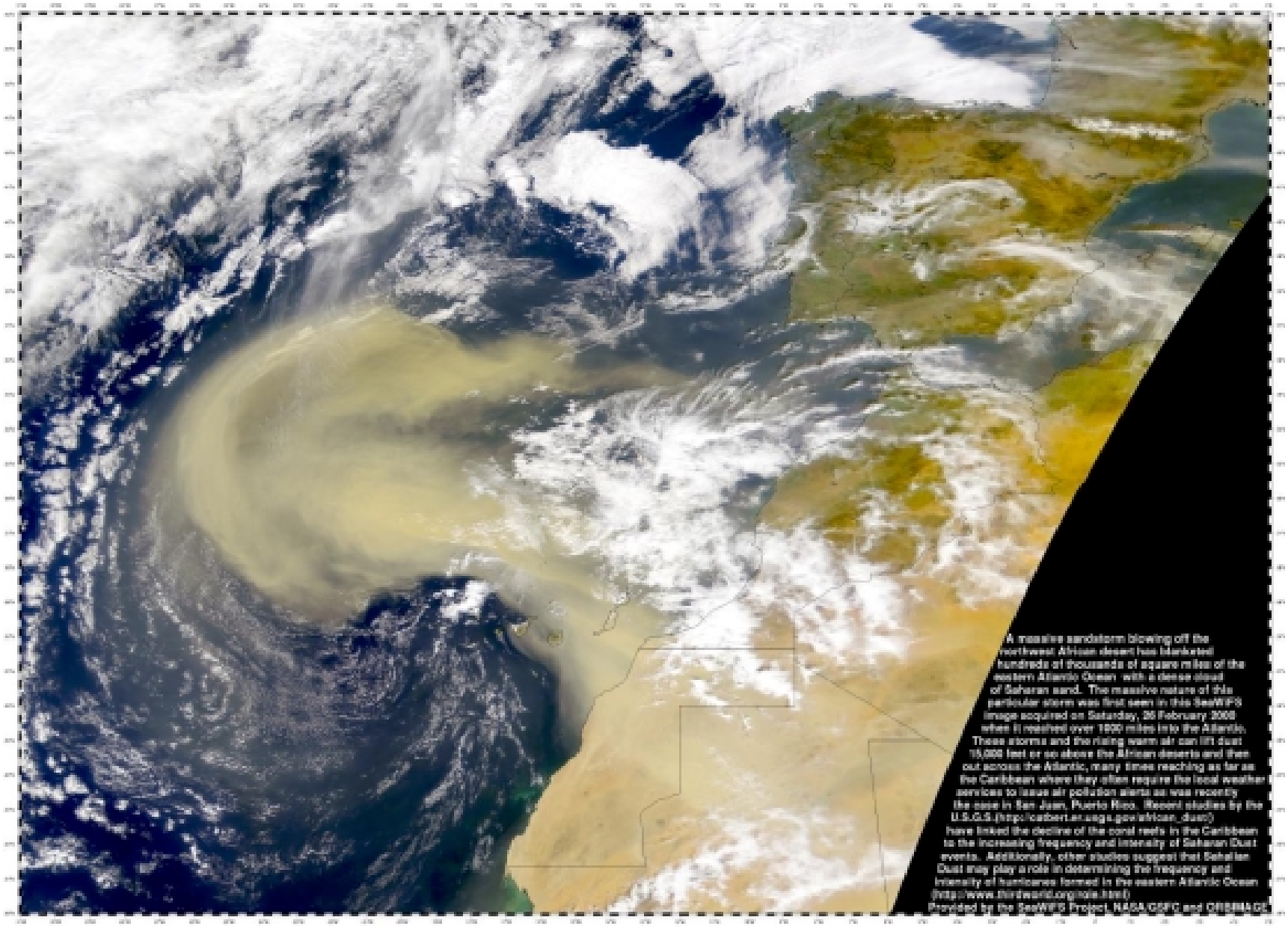

Figure 4: **SeaWIFS image of Sharan Dust Blowing off African Coast.**

Airborne dust (brown haze) over the Caribbean Sea. This dust originated in the Sahara Desert of western Africa where it was lifted and carried off the coast by strong winds.

CREDIT: NOAA

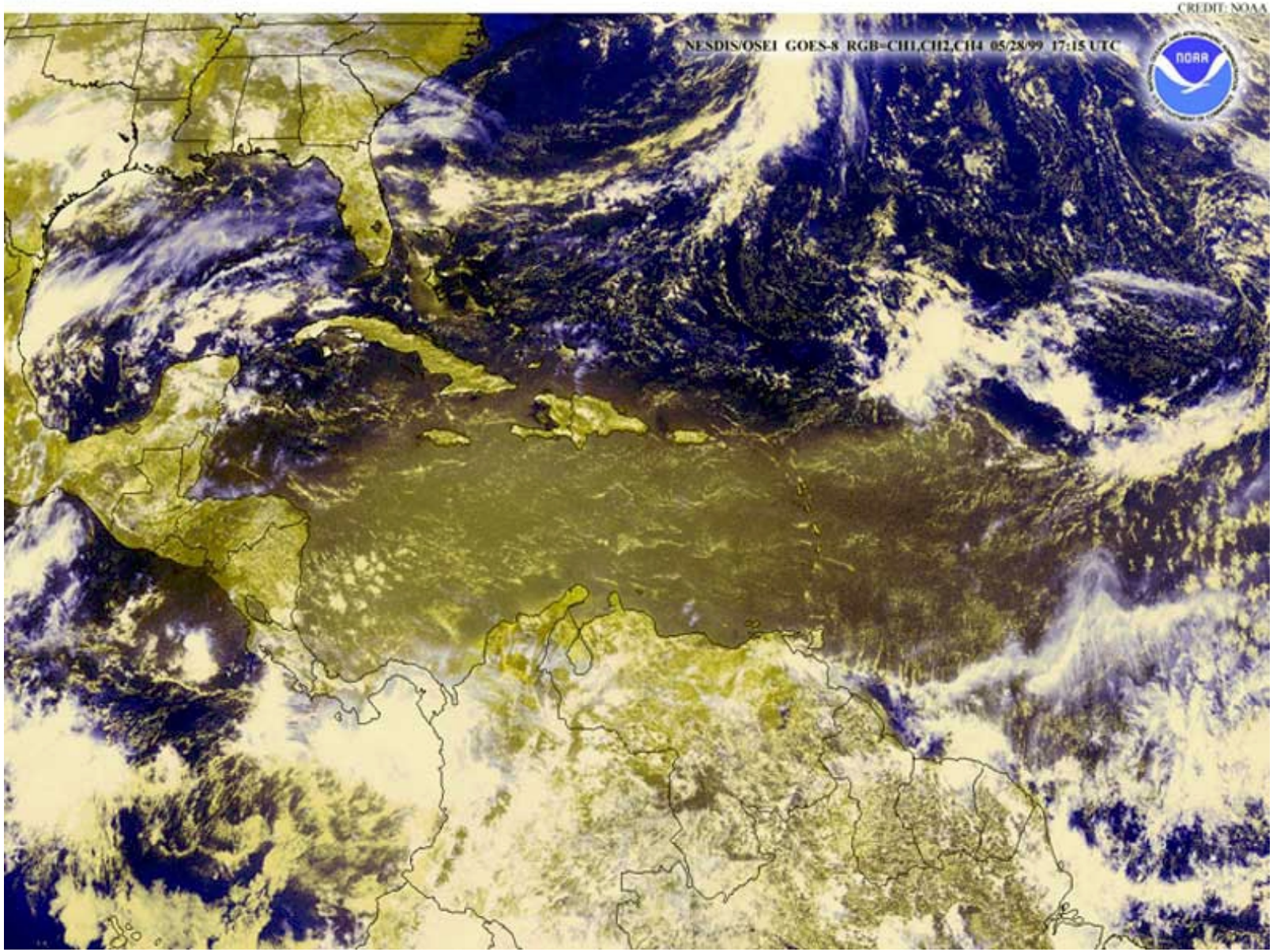

Figure 5: **SeaWIFS image of Sharan Dust over the Carribean.**

Review of the SeaWiFS Algorithm – (1)

The current SeaWiFS ocean color algorithm includes two distinct steps:

- First, "atmospheric correction" is performed to obtain the water-leaving radiance.
- Second, the oceanic chlorophyll concentration is retrieved from this water-leaving radiance.

In the visible more than 90% of the radiance measured by the satellite sensor typically comes from the atmosphere. This makes atmospheric correction important because:

- a small uncertainty in the atmospheric correction may lead to a big error in the inferred chlorophyll concentration;
- optical properties vary considerably in space and time.

Review of the SeaWiFS Algorithm – (2)

Assuming that the effects of sun glitter and white caps have been removed, we may express the satellite-measured reflectance as:

$$\rho_{tot}(\lambda) = \rho_{path}(\lambda) + t(\lambda)\rho_w(\lambda), \tag{27}$$

where

$t(\lambda)$ = **diffuse transmittance,**
$\rho_w(\lambda)$ = **water-leaving reflectance, and**
$\rho_{path}(\lambda)$ = **contribution from the atmosphere:**

$$\rho_{path}(\lambda) = \rho_{ray}(\lambda) + \rho_{aero}(\lambda) + \rho_{ra}(\lambda). \tag{28}$$

The three terms are due to multiple scattering:

$\rho_{ray}(\lambda)$ => **by air molecules alone;**
$\rho_{aero}(\lambda)$ => **by suspended atmospheric particles alone;**
$\rho_{ra}(\lambda)$ => **by simultaneous presence of molecules and aerosols.**

Review of the SeaWiFS Algorithm – (3)

In the single scattering approximation $\rho_{ra} = 0$, and $\rho_{aero}(\lambda) \approx \rho_{as}(\lambda)$. Thus, Eq. (28) may be rewritten as:

$$\rho_{as}(\lambda) = \rho^{ss}_{path}(\lambda) - \rho_{ray}(\lambda) \tag{29}$$

where $\rho^{ss}_{path}(\lambda)$ is the single scattering approximation to $\rho_{path}(\lambda)$.

However, the aerosol contribution to the reflectance $\rho_{as}(\lambda)$ may be determined (Gordon, 1996; 1997) from:

$$\rho_{as}(\lambda) = \omega_a(\lambda)\tau_a(\lambda)p_a(\theta, \phi, \theta_0, \phi_0; \lambda)/4\cos\theta\cos\theta_0. \tag{30}$$

Here:

- ω_a **is the aerosol single scattering albedo,**
- p_a **takes into account the single scattering by aerosol particles as well as the Fresnel reflection by the underlying ocean.**
- **For a given aerosol model, ω_a and p_a are known: τ_{865} is estimated from a pre-computed lookup table of ρ_{as}.**

Review of the SeaWiFS Algorithm – (4)

The SeaWiFS algorithm employs the parameter:

$$\epsilon_{ss}(\lambda, 865) = \rho_{as}(\lambda)/\rho_{as}(865) \tag{31}$$

and

$$\epsilon_{ss}(765, 865) = \rho_{as}(765)/\rho_{as}(865)$$

is used to select

- **the two aerosol models among 12 candidate models that have ϵ-values closest to the correct value. BUT**
- **the parameter $\epsilon_{ss}(765, 865)$ cannot be obtained directly from the satellite-observed radiances.**

In order to generalize this approach to include multiple scattering effects, Gordon and Wang (1994) introduced a correction factor:

$$\rho_{path}(\lambda) - \rho_{ray}(\lambda) = \rho_{aero}(\lambda) + \rho_{ra}(\lambda) \equiv K[\lambda, \rho_{as}(\lambda)]\rho_{as}(\lambda). \tag{32}$$

Review of the SeaWiFS Algorithm – (5)

The following procedure is used to determine $\epsilon_{ss}(765, 865)$ and then the aerosol model:

- **Start by computing the average ϵ_{ss}^{ave} for the 12 candidate aerosol models assuming that the K^j-value for each model is correct, i.e.:**

$$\epsilon_{ss}^{ave}(765, 865) = \frac{1}{N} \sum_{j=1}^{N=12} {\epsilon_{ss}}^{j}(765, 865) \tag{33}$$

with

$$ {\epsilon_{ss}}^{j}(765, 865) = \frac{{\rho_{as}}^{j}(765)}{{\rho_{as}}^{j}(865)} = \frac{K^j[865, \rho_{as}(865)]}{K^j[765, \rho_{as}(765)]} [\frac{\rho_{aero}(765) + \rho_{ra}(765)}{\rho_{aero}(865) + \rho_{ra}(865)}] \tag{34}$$

where the superscript j denotes the candidate aerosol model, and

- **$\rho_{aero}(765) + \rho_{ra}(765)$ and $\rho_{aero}(865) + \rho_{ra}(865)$ are computed from the satellite-observed radiance using $\rho_{path}^{mea}(\lambda) - \rho_{ray}(\lambda)$ [see Eq. (28)] with λ = 765 and 865 nm, respectively.**

Review of the SeaWiFS Algorithm – (6)

Then:

- **discard the two models with the largest positive values of ϵ_{ss}^{ave} - ϵ_{ss}^{j} as well as the two models with the largest negative values, and proceed to compute a new average of ϵ^{ave}.**

Repeat procedure until one ϵ_{ss}^{ave}-value and only two models remain:

- **one with ϵ_{ss}^{ave} - $\epsilon_{ss}^{j} > 0$ and one with ϵ_{ss}^{ave} - $\epsilon_{ss}^{j} < 0$.**

To derive $\epsilon_{ss}(\lambda, 865)$ and $\rho_a(\lambda) + \rho_{ra}(\lambda)$ at visible wavelengths from $\epsilon_{ss}^{ave}(765, 865)$ it is assumed that:

(i) $\epsilon_{ss}(\lambda, 865)$ falls between the same two aerosol models as $\epsilon_{ss}^{ave}(765, 865)$,

(ii) $K[\lambda, \rho_{as}(\lambda)]$ falls between the two values for these models in the same proportion as $\epsilon_{ss}^{ave}(765, 865)$.

Review of the SeaWiFS Algorithm – (7)

After values $\epsilon_{ss}(\lambda, 865)$ at visible wavelengths are obtained:

$$\rho_{as}(\lambda) = \epsilon_{ss}(\lambda, 865)\rho_{as}(865) \tag{35}$$

and, $\rho_a(\lambda) + \rho_{ra}(\lambda)$ at visible wavelengths is computed from:

$$\rho_a(\lambda) + \rho_{ra}(\lambda) = K[\lambda, \rho_{as}(\lambda)]\rho_{as}(\lambda). \tag{36}$$

- **Lookup tables are created for $K[\lambda, \rho_{as}(\lambda)]$ for each of the 12 candidate aerosol models for several values of θ_0 and θ_v.**
- **For a specific set of (θ_0, θ_v) a least squares fit is obtained as follows:**

$$\log_e \left\{K[\lambda, \rho_{as}(\lambda)]\rho_{as}(\lambda)\right\} = \log_e a_1(\lambda) + a_2(\lambda) \log_e[\rho_{as}(\lambda)] + a_3(\lambda) \log_e^2[\rho_{as}(\lambda)].$$

- **The azimuth-dependence of the coefficients a_i is expanded in a Fourier series in θ_v using 14 terms.**

Review of the SeaWiFS Algorithm – (8)

Finally, by subtracting $\rho_{path}(\lambda)$ from the measured reflectance $\rho_{tot}(\lambda)$ [Eq. (27)] and dividing by $t_v(\lambda)$, the atmospheric diffuse transmittance along the path towards the satellite, one obtains:

- **the normalized water-leaving reflectance at visible wavelengths, $[\rho_w(\lambda)]_N$, defined as:**

$$[\rho_w(\lambda)]_N = \rho_w(\lambda)/t_0(\lambda) = [\rho_{tot}(\lambda) - \rho_{path}(\lambda)]/[t_0(\lambda)t_v(\lambda)], \tag{37}$$

where $t_0(\lambda)$ is the diffuse transmittance along the solar beam path.

- **Pre-computed atmospheric transmittances $t_v(\lambda)$ and $t_0(\lambda)$ are used to obtain the normalized water-leaving reflectance $[\rho_w(\lambda)]_N$.**

Note that in the SeaWiFS algorithm:

- **all computations are done using a two-layer atmosphere: molecules only in the upper layer; aerosols only in the lower layer.**

Review of the SeaWiFS Algorithm – (8)

Then:

- **the chlorophyll concentration is estimated from a two-band ratio $R_{12}(\lambda) = [\rho_w(\lambda)]_N/[\rho_w(555)]_N$ according to an empirical relation derived by statistical regression (O'Reilly, 1998):**

$$\text{Ratio} = Max[R_{12}(443), R_{12}(490), R_{12}(510)]; \tag{38}$$

$$\log R = \log_{10}(\text{Ratio})$$

$$C = 10^{0.366 - 3.067 \log R + 1.930 \log R^2 + 0.649 \log R^3 - 1.532 \log R^4}.$$

The coefficients in this empirical formula were derived from field-measured reflectance data compiled in the SeaBAM database.

Review of the SeaWiFS Algorithm – (9)

In summary, the SeaWiFS algorithm works as follows:

1. It employs the single scattering approximation (SSA) with a multiple scattering correction using a two-layer atmosphere.
2. It employs the near-infrared black-pixel approximation.
3. It retrieves "aerosol model" and τ_{865} from the SSA.
4. It employs the retrieved "aerosol model" and τ_{865} to infer the atmospheric contribution to the TOA radiance in the visible.
5. It subtracts this atmospheric contribution from the measured radiance to obtain TOA water-leaving radiance in the visible.
6. It employs two approximate atmospheric transmittances to obtain surface normalized water-leaving radiance in the visible.
7. It employs normalized water-leaving radiance (assumed to be isotropic) to infer chlorophyll concentrations from regressions.

Review of the SeaWiFS Algorithm – (10)

The SeaWiFS algorithm contains many assumptions leading to uncertainties that are difficult if not impossible to quantify:

1. Use of a two-layer model and SSA to infer aerosol optical depth.
2. Use of an approximate multiple scattering correction.
3. Use of the black-pixel approximation. An attempt to remedy this problem (Siegel et al., 2000) is based on an approximate reflectance model.
4. Use of the assumption that the water-leaving radiance is isotropic over the upward hemisphere.
5. Use of the assumption that the atmospheric and oceanic radiative transfer problems are decoupled.
6. Use of two approximate transmittances to infer the normalized water-leaving radiance (at the surface) from the TOA water-leaving radiance.

New Algorithm – (1)

Goal:

- Remove unnecessary assumptions invoked in the SeaWiFS algorithm that lead to uncertainties that are difficult to quantify.

In addition to the assumptions listed above Gordon (1997) states:

- the expansion of the azimuth-dependence of the radiance in a Fourier series in θ_v using 14 terms yields about the same accuracy as an interpolation with a division in θ_v of 5° or 10°. However:
- our experience is that such interpolation in azimuth yields insufficient accuracy. We use a more accurate approach.

To remove these uncertainties our algorithm is based on DISORT:

- a rigorous discrete-ordinates solution of the radiative transfer equation pertinent for the coupled atmosphere-ocean system.

New Algorithm – (2)

DISORT (Stamnes et al., 1988; Thomas and Stamnes, 1999) was extended by Jin and Stamnes (1994) to apply to:

- the coupled atmosphere-ocean (CAO) system and further extended by Yan and Stamnes (2002) to yield the radiance at arbitrary polar angles. The resulting:
- CAO-DISORT code yields accurate radiances (reflectances) at any polar and azimuth angles (the satellite viewing angles), and at any desired level in the atmosphere-ocean system.

In short the CAO-DISORT method works as follows:

1. The atmosphere-ocean system is treated as two adjacent slabs separated by an interface across which the index of refraction changes from $m_r \approx 1$ in the air to $m_r \approx 1.33$ in the water.
2. Each of the two slabs is divided into a sufficient number of layers to adequately resolve the variation of the inherent optical properties with altitude in the air and depth in the ocean.

New Algorithm – (3)

3. The interface between the atmosphere and the ocean is treated as a flat surface (assuming that effects of sun glitter and white caps have been removed), the reflection and transmission through the interface are computed by Fresnel's equations, and the bending of the rays across the interface follows Snell's law.
4. The radiative transfer equation is solved separately for each layer in the atmosphere and ocean using the discrete-ordinate method.
5. The solution is completed by applying boundary conditions at the top of the atmosphere and bottom of the ocean as well as appropriate radiance ($I(\tau, u, \phi)$) continuity conditions (I/m_r^2 is a conserved quantity) at the layer interfaces in the atmosphere and ocean, and at the air-ocean interface (where Fresnel's equations apply).

New Algorithm – (4)

As a part of the solution procedure, the radiance is expanded in a Fourier cosine series:

$$I(\tau, \mu_v, \mu_0, \Delta\phi) = \sum_{m=0}^{2M-1} I^m(\tau, \mu_v, \mu_0) \cos m\Delta\phi, \tag{39}$$

where

$\mu_v = \cos\theta_v$ **is the cosine of the polar (viewing) angle** θ_v**,**

$\mu_0 = \cos\theta_0$ **is the cosine of the solar zenith angle** θ_0**,**

$\Delta\phi = \phi_0 - \phi_v$ **is the relative azimuth angle between the incident solar beam azimuth** ϕ_0 **and the sensor viewing azimuth** ϕ_v**,**

$I(\tau, \mu_v, \mu_0, \Delta\phi)$ **is the radiance, and**

$I^m(\tau, \mu_v, \mu_0)$ **is the** m^{th} **Fourier component of the radiance.**

Each Fourier component satisfies a radiative transfer equation whose solution yields $I^m(\tau, \mu_v, \mu_0)$**, and substitution in Eq. (39) yields** $I(\tau, \mu_v, \mu_0, \Delta\phi)$**.**

New Algorithm – (5)

We store the Fourier components $I^m(\tau = 0, \mu_v, \mu_0)$ in a lookup table

- **and use cubic spline interpolation to compute them for the angles corresponding to a specific sun-satellite geometry. Then**
- **$I(\tau = 0, \mu_v, \mu_0, \Delta\phi)$ is computed from Eq. (39), which yields an accurate analytic treatment of the ϕ-dependence of the radiance.**

In our lookup tables we store:

- **19 azimuthal components, and each of them is pre-computed at 11 polar (viewing) angles, θ_{vi}, and 14 solar zenith angles, θ_{0i}.**

This provides a grid structure that we use to interpolate:

- **reflectances to a specific pair of polar viewing angle θ_v and solar zenith angle θ_0 required by the sun-satellite geometry, which:**
- **yields a TOA reflectance precision better than 1% compared to direct computations with the CAO-DISORT model.**

New Algorithm – (6)

Our atmospheric correction differs from the SeaWiFS approach in two major ways. In our algorithm:

1. **the aerosol optical properties are computed in a more realistic manner (Yan et al., 2002);**
2. **our retrieval of aerosol information, and extrapolation from the NIR to the visible is more accurate because it is based on:**
   - **accurate and self-consistent treatment of the multiple scattering process;**
   - **accurate computation of the Fourier components of the radiance, $I^m(\tau = 0, \mu_{vi}, \mu_{0i})$, stored in the look-up tables;**
   - **accurate interpolation to obtain the Fourier components of the radiance, $I^m(\tau = 0, \mu_v, \mu_0)$, at the actual sun-satellite geometry;**
   - **accurate, analytic treatment of the azimuth-dependence of the radiance: $I(\tau, \mu_v, \mu_0, \Delta\phi) = \Sigma_{m=0}^{2M-1} I^m(\tau, \mu_v, \mu_0) \cos m\Delta\phi$.**

New Algorithm – (7)

The aerosol optical properties may be computed in two different ways:

1. SeaWiFS relies on a single-component (SC) approach:

   - combine aerosol species with different chemical compositions and hygroscopicities into an effective "pseudoparticle" by computing an average refractive index of the mixture.
   - This "pseudoparticle" is then allowed to grow and change its refractive index with increasing humidity, and Mie theory is applied to compute its optical properties.

1. We adopt a more realistic multi-component (MC) approach:

   - aerosol components with different compositions and hygroscopicities are treated separately; each component is allowed:
   - to grow and change its refractive index independently with increasing humidity. Optical properties of each component: from Mie theory; mixture: use concentration-weighted average.

Light and Life STEVENS Institute of Technology Laboratory

New Algorithm – (8)

Yan et al. (2002), comparing results computed by the MC approach with those computed by the SC approach, found that:

- when the relative RH $> 90\%$, difference between SC and MC approaches: $\Delta\rho^{TOA} > \rho_w$, the water-leaving radiance. BUT if we:
- restrict ourselves to low RH: aerosol properties computed by SC approach (SeaWiFS algorithm) will not be significantly different from those computed by MC approach (our algorithm).

Therefore, to compare and explore possible differences between our new methodology and the SeaWiFS methodology, due to causes other than use of different aerosol IOPs, we may select:

- the Maritime and Tropospheric aerosol models both at relative humidity RH $= 50\%$ (M-50 and T-50) as suitable candidates for exploring the retrieval capabilities (aerosol properties and chlorophyll concentrations) of both SeaWiFS and our algorithm.

New Algorithm – (9)

Our atmospheric correction algorithm employs two parameters to select an aerosol model from a suite of candidate models and to retrieve the corresponding aerosol optical depth:

$$\epsilon_{ms}(\lambda, 865) = [\rho_{path}(\lambda) - \rho_{ray}(\lambda)]/[\rho_{path}(865) - \rho_{ray}(865)]. \quad (40)$$

and

$$\gamma_{diff}(\lambda, 865) = \gamma(\lambda) - \gamma(865) \quad (41)$$

where $\gamma(\lambda) = \rho_{path}(\lambda)/\rho_{ray}(\lambda)$.

We use $\epsilon_{ms}(765, 865)$ **to retrieve the aerosol model and** $\gamma_{diff}(765, 865)$ **to retrieve the aerosol optical depth** τ_{865}**, because:**

- $\epsilon_{ms}(765, 865)$ **is very sensitive to the aerosol model but insensitive to the aerosol optical depth as illustrated in Fig. 6.**
- $\gamma(\lambda)$ **is insensitive to the vertical distribution of the aerosols, even for strongly absorbing aerosols (Antoine and Morel, 1999).**

New Algorithm – (10)

As shown in Fig. 6:

- **all the non-absorbing or weakly absorbing aerosols yield almost identical γ_{diff}-values, whereas the absorbing (urban) aerosols lead to a distinctly different behavior. Thus:**
- **γ_{diff} is potentially useful for distinguishing absorbing aerosols from non-absorbing or weakly absorbing ones.**

Note that in our new algorithm the parameters:

- **ρ_{tot}, ρ_{path}, and ρ_{ray} in Eqs. (1) and (2) are computed accurately by the CAO-DISORT code, and that $t\rho_w$ is obtained by subtraction:**

$$t\rho_w = \rho_{tot} - \rho_{path}.$$

New Algorithm – (11)

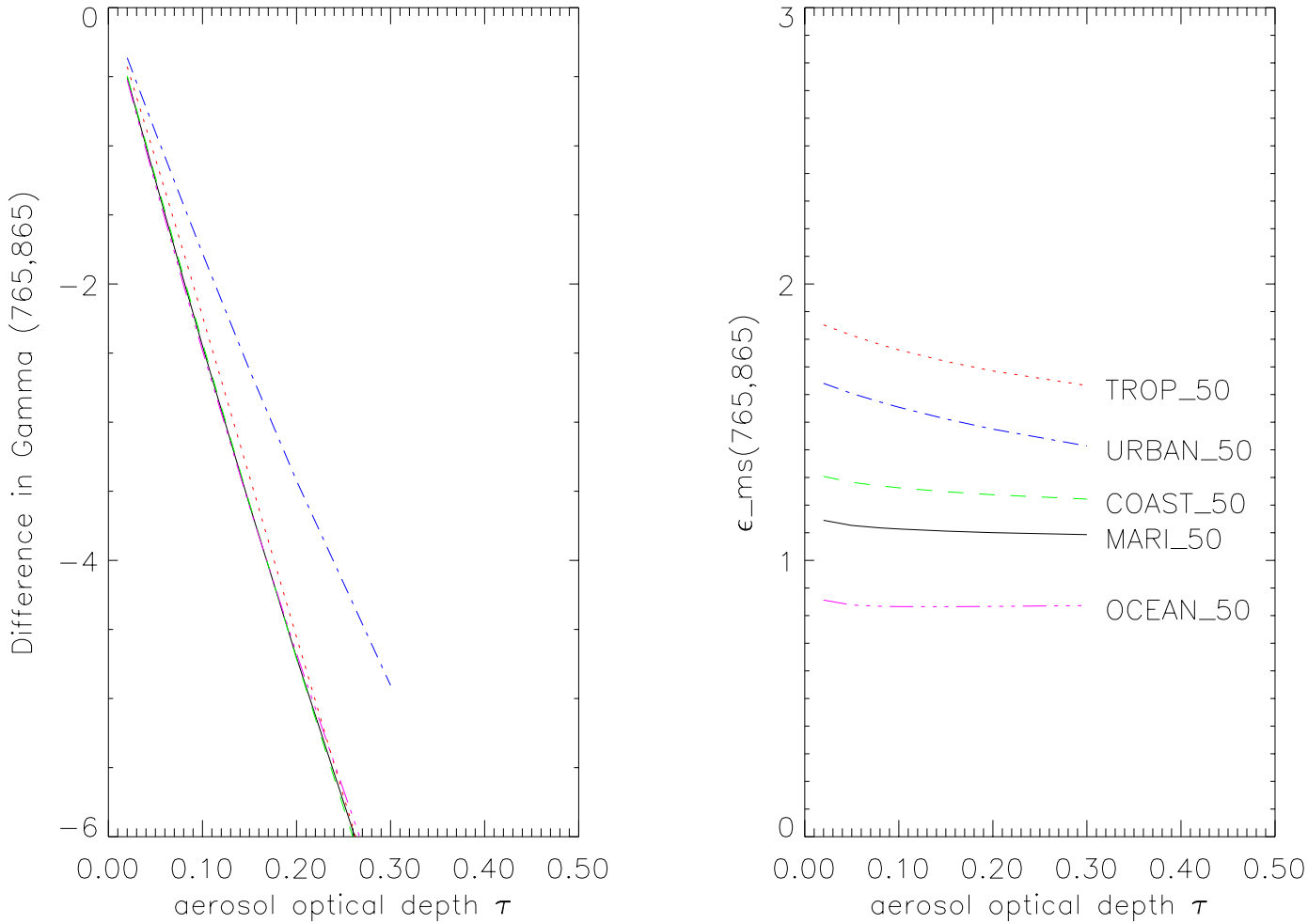

Figure 6: **Simulated values of $\gamma_{diff}(765, 865)$ and $\epsilon_{ms}(765, 865)$ as a function of aerosol optical depth τ_{865} for several aerosol models including maritime, tropospheric, coastal, urban, and oceanic at RH = 50%. The various aerosol models in the left panel are labeled in the same way as indicated in the right panel.**

New Algorithm – (12)

In the aerosol retrieval process, we start by using:

- $\gamma_{diff}(765, 865)$ **to retrieve the aerosol optical depth** τ_{865} **for each of the candidate aerosol models. We then use:**
- $\epsilon_{ms}(765, 865)$ **to pick the most appropriate aerosol model from 20 candidate aerosol models, representing different aerosol types.**
- **For each aerosol model, pre-computed TOA reflectances** ρ_{path} **and** ρ_{tot} **are stored in look-up tables for rapid access by the algorithm.**
- **We store reflectances for** $\tau_{865} =$ **0., 0.02, 0.05, 0.08, 0.1, 0.15, 0.2, 0.3; use interpolation to obtain radiances at arbitrary** τ_{865}**-values, and** $\rho_{path}(\lambda) - \rho_{ray}(\lambda) = \epsilon_{ms}(\lambda, 865)[\rho_{path}(865) - \rho_{ray}(865)]$ **(Eq. (40))**
- **to extrapolate the aerosol contribution to the TOA radiance from the NIR to the visible spectral range.**

New Algorithm – (13)

Chlorophyll Concentration Retrieval:

We use the CAO-DISORT code to compute the TOA radiance assuming that the inherent optical properties (IOPs) of the ocean can be described by a single homogeneous layer of Case I waters. The IOP model consists of:

1. the absorption coefficient $a_w(\lambda)$ for pure seawater measured by Pope and Fry (1997);
2. the scattering coefficient for pure seawater $b_w(\lambda)$ tabulated by Smith and Baker (1981);
3. the absorption coefficient $a_c(\lambda)$ for chlorophyll pigments parameterized in terms of the chlorophyll concentration by the method of Morel and Maritorena (2001);
4. the volume scattering function for particles measured by Petzold (1972);
5. the scattering coefficient $b_c(\lambda)$ parameterized in terms of the chlorophyll concentration (Li and Stamnes, 2001).

New Algorithm – (14)

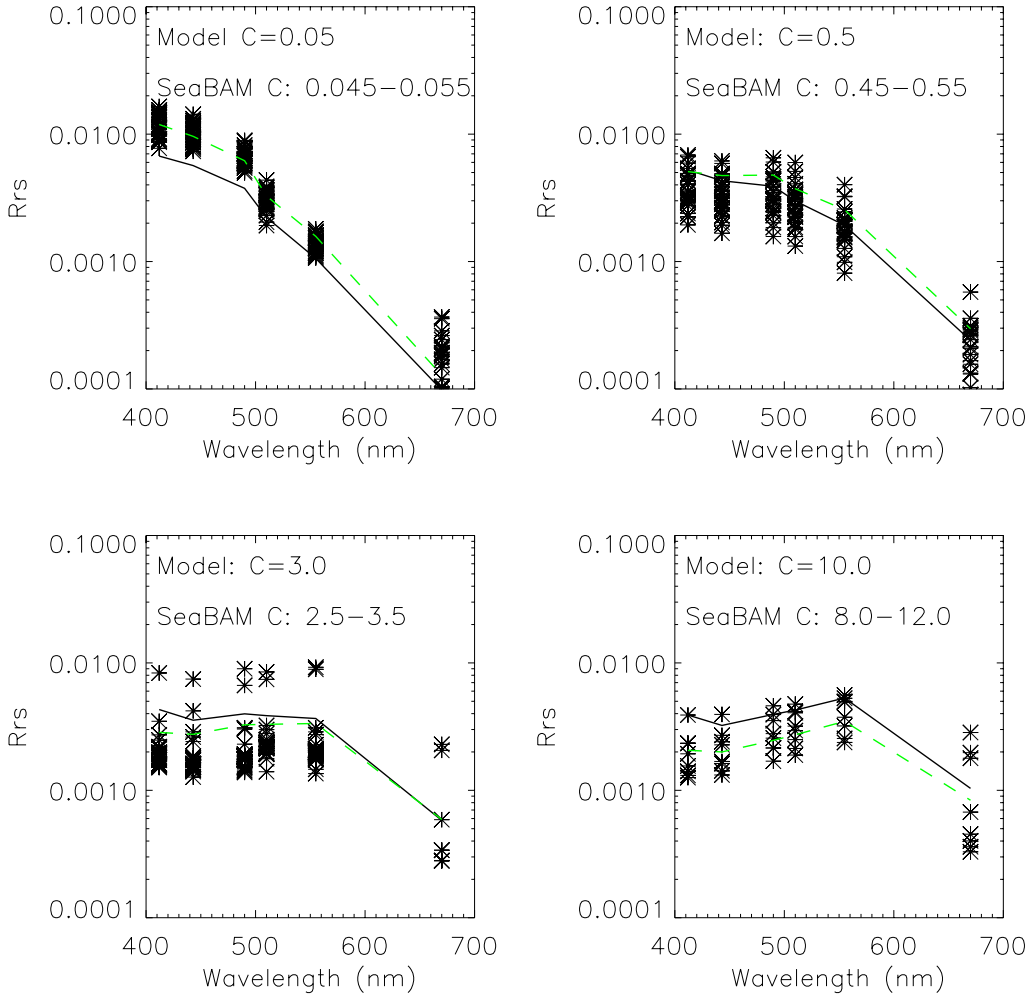

Figure 7: **Comparisons between R_{rs} values computed from a radiative transfer model for the coupled atmosphere-ocean system and R_{rs} values from the SeaBAM data base for similar chlorophyll concentrations. Solid lines and dashed lines are the computed R_{rs} values based on the "old" Morel bio-optical model and the "new" modified Morel model, respectively. The stars represent the measured R_{rs} values provided in the SeaBAM data base.**

New Algorithm – (15)

Li and Stamnes (2001) found that:

- **the above IOP model with $b_c(\lambda) = 0.35C^{0.50}(550/\lambda)$ provided a good overall match between remote sensing reflectances computed with CAO-DISORT and determined from the SeaBAM database.**

This bio-optical IOP model is used in CAO-DISORT:

- **to compute the reflectance ρ_{path}^{comp} accurately by taking the coupling between the atmosphere and the ocean into account.**

Precision of radiances retrieved from lookup tables is very high:

- **the path radiance retrieved from them ρ_{path}^{retr} will be very accurate, that is $\rho_{path}^{retr} \approx \rho_{path}^{comp}$. The TOA water-leaving reflectance $t\rho_w$ is obtained by subtracting ρ_{path}^{retr} from the measured reflectance ρ_{tot}^{meas}: $t\rho_w = \rho_{tot}^{meas} - \rho_{path}^{retr}$, and we use the ratio:**

$R_w = t(\lambda_1)\rho_w(\lambda_1)/t(\lambda_2)\rho_w(\lambda_2)$ to retrieve chlorophyll concentration, where $\lambda_1 = 490$ nm and $\lambda_2 = 555$ nm (see Fig. 8).

New Algorithm – (16)

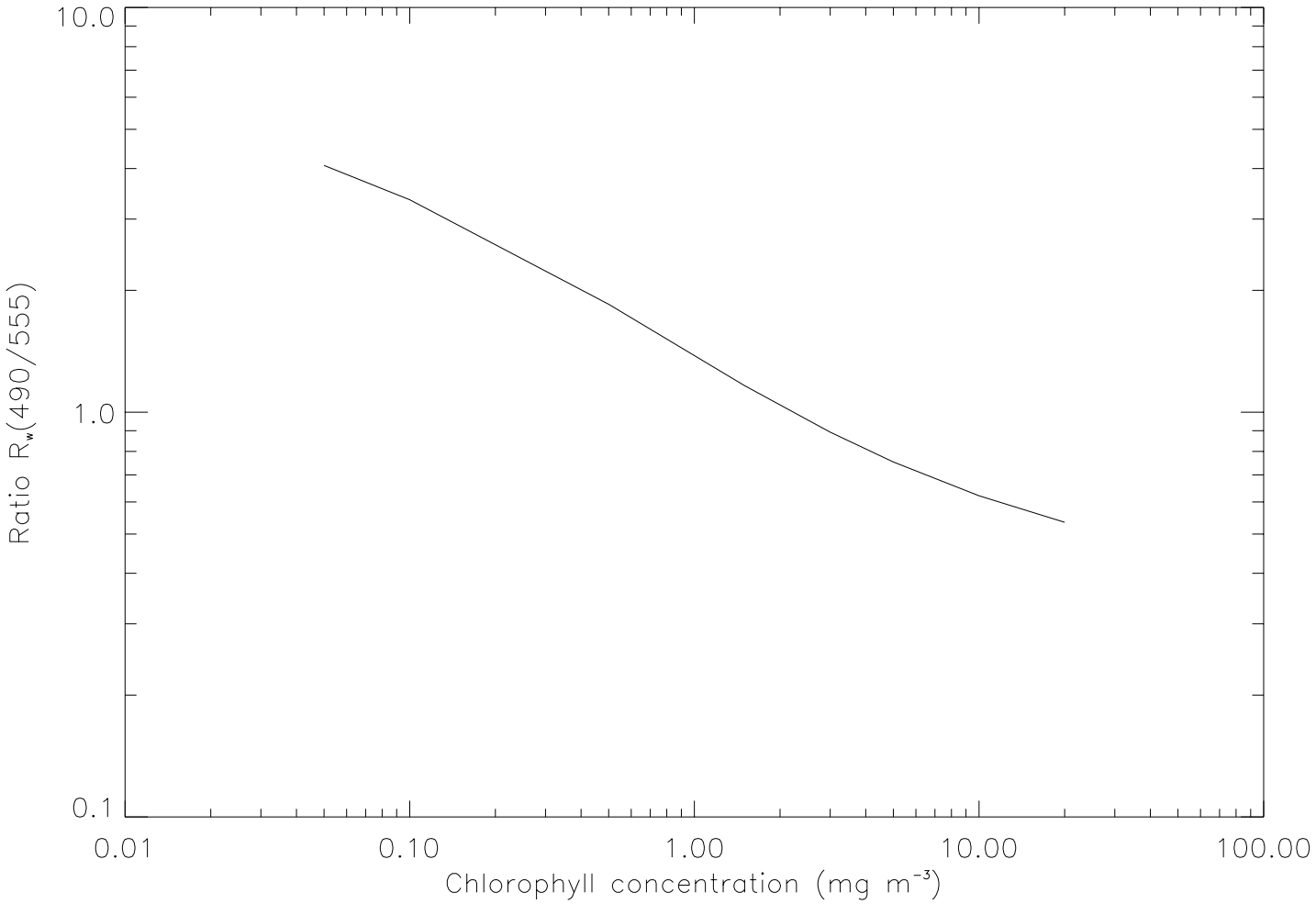

Figure 8: **Plot of $R_w = t(490)\rho_w(490)\ /\ t(555)\rho_w(555)$ versus chlorophyll concentration for the Maritime aerosol model (RH=50%) with an aerosol optical depth of $\tau = 0.1$.**

New Algorithm – (17)

In summary, the main differences between the two algorithms for chlorophyll concentration retrieval are:

1. Our approach relies on the use of a bio-optical IOP model in conjunction with a comprehensive radiative transfer model. An empirical approach is used in the SeaWiFS algorithm, although a bio-ptical model is employed to relax the NIR black-pixel assumption in the atmospheric correction process.
2. We use TOA water-leaving reflectances to retrieve the chlorophyll concentration, whereas the SeaWiFS algorithm relies on the use of surface normalized water-leaving reflectances.
3. The SeaWiFS algorithm relies on an empirical formula for retrieval of chlorophyll concentrations based on the assumption that the water-leaving radiance is isotropic. Our algorithm employs the TOA water-leaving reflectance, which is self-consistently, and accurately retrieved from the lookup tables for the actual sun-satellite geometry.

New Algorithm – (18)

Using CAO-DISORT combined with the IOP model, we developed an iterative method for:

- **simultaneous retrieval of the chlorophyll concentration C and the aerosol optical properties.**
- **The implementation steps of this algorithm are as follows:**

Step 1: Pick an initial chlorophyll concentration C_0. Use $\epsilon_{ms}(555, 865)$ and $\gamma_{diff}(555, 865)$ to retrieve an aerosol model and the corresponding τ_{865}. Then go to Step 2. Note: we use the channels at 555 nm (instead of 765 nm) and 865 nm to pick the initial aerosol model and corresponding τ_{865} because the radiance at 555 nm is relatively insensitive to the initial chlorophyll concentration.

Step 1': Use the retrieved chlorophyll concentration C, and $\epsilon_{ms}(765, 865)$ and $\gamma_{diff}(765, 865)$ to retrieve an aerosol model and the corresponding τ_{865}. Go to Step 2.

New Algorithm – (19)

Step 2: Use the retrieved aerosol model and τ_{865} to extrapolate $\rho_{path}(\lambda)$ from the NIR to the visible, and to determine $t\rho_w(\lambda) = \rho_{tot}^{meas}(\lambda) - \rho_{path}^{extrap}(\lambda)$ at $\lambda = 490$ and 555 nm.

Step 3: Estimate the chlorophyll concentration C from $t(490)\rho_w(490)/t(555)\rho_w(555)$.

Step 4: Repeat steps 1'-3 with retrieved C, until a converged set of aerosol optical properties and chlorophyll concentration C is obtained.

Typically, 2–3 iterations are sufficient to retrieve a converged set of aerosol optical properties and chlorophyll concentration.

New Algorithm – (20)

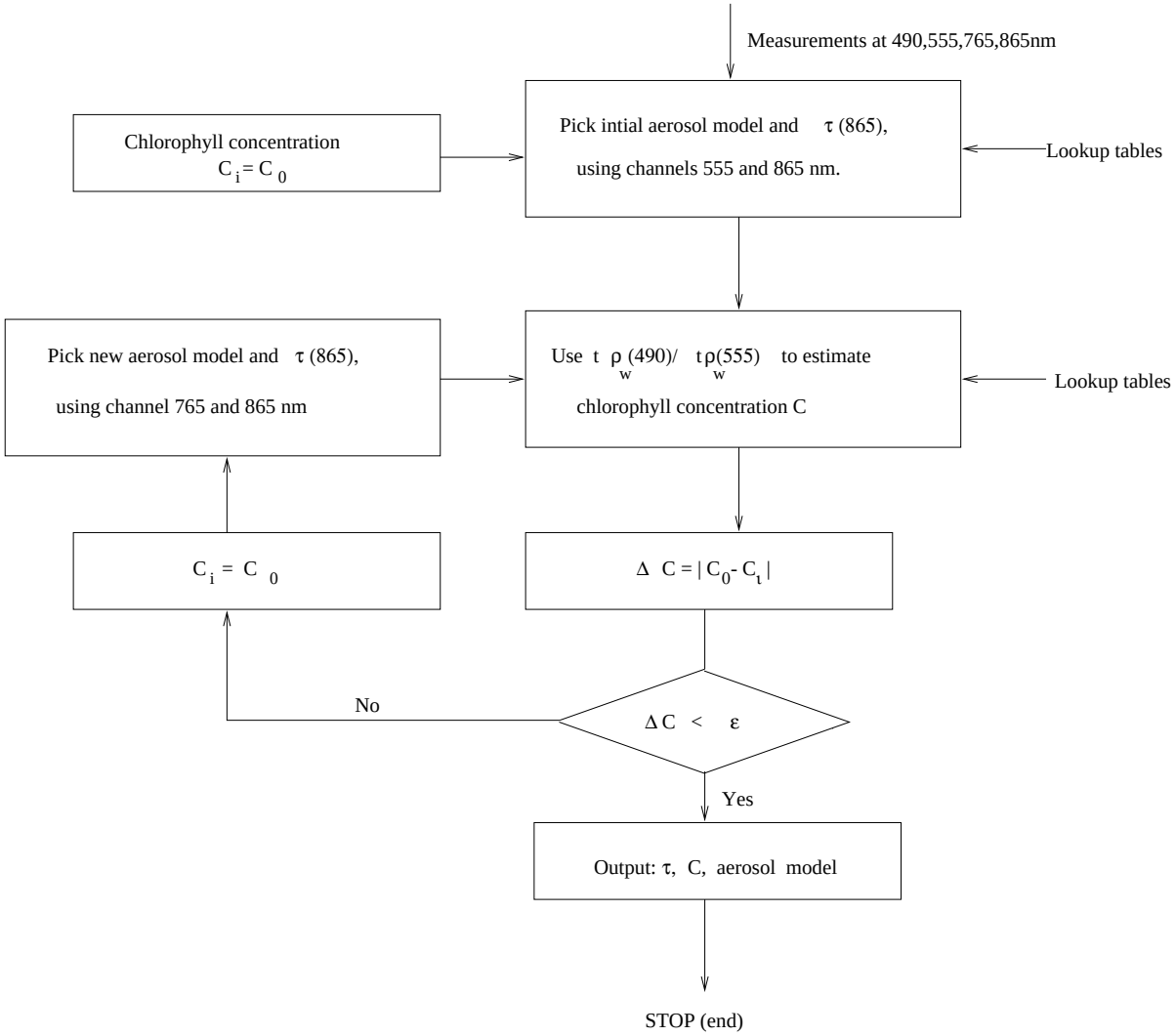

Figure 9: **Flow chart of the algorithm for simultaneous retrieval of aerosol optical properties and chlorophyll concentration.**

Evaluation – (1): Testbed

In order to evaluate our new algorithm we designed:

- a numerical testbed aimed at testing its ability to achieve simultaneous retrieval of atmospheric aerosol properties and oceanic chlorophyll concentration. Using CAO-DISORT:
- we constructed a series of "synthetic" TOA radiances for many combinations of aerosol properties ("model" and τ_{865}) and C.

We then applied the retrieval algorithm to this synthetic data set to answer the question:

- how well can we retrieve the aerosol "model" and τ_{865} as well as the chlorophyll concentration C from the synthetic radiances?

By comparing the retrieved results with the input data used to create the synthetic ("measured") radiances, we can judge:

- the retrieval capability of both the SeaWiFS and our algorithm on the same synthetic data set, and compare their relative merits.

Evaluation – (2): Aerosol retrieval

We consider two test cases by simulating "measured" radiances:

1. **We used the M-50 aerosol model with τ_{865} = 0.02, 0.05, 0.08, 0.1, 0.15, 0.2, 0.3, and C = 0.05, 0.1, 0.5, 1.5, 3.0, 5.0, 10.0, 20.0 mg·m^{-3}.**
2. **We used the same values of τ_{865} and C, but we picked the T-50 instead of the M-50 aerosol model.**

Sun-satellite geometry chosen for the simulated testbed data set:

- **was a solar zenith angle of $\theta_0 = 34.5^0$, a viewing zenith angle of $\theta = 51.25^0$, and a relative azimuth angle of $\Delta\phi = 120^0$.**

Due to different treatments of ozone and oxygen A-band corrections in the two algorithms, we decided to ignore the effects of:

- **ozone and oxygen A-band absorption in both the simulated testbed data and the retrieval algorithms: Focus is on: retrieval of aerosol "model" and τ_{865} and C.**

Evaluation – (3): Aerosol retrieval

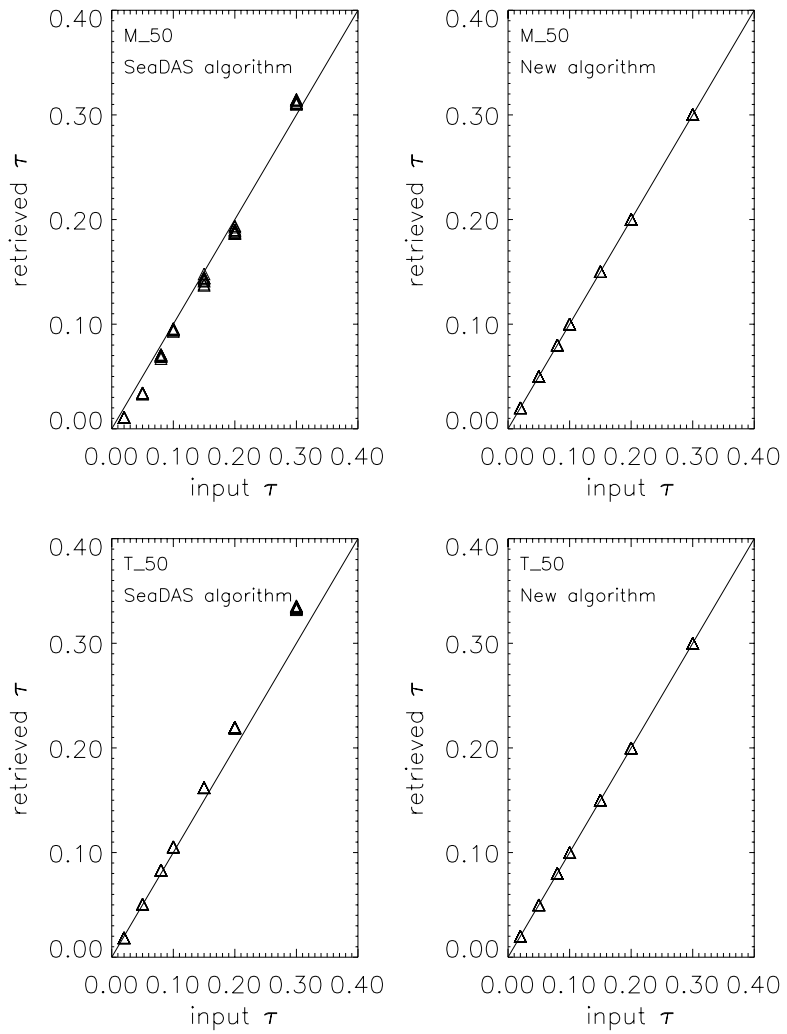

Figure 10: **Retrieved aerosol optical depth at 865 nm compared to the input value. The top panels pertain to the M-50 aerosol model, and the bottom ones to the T-50 aerosol model. Left panels: SeaWiFS algorithm. Right panels: New algorithm.**

Evaluation – (4): Chlorophyll retrieval

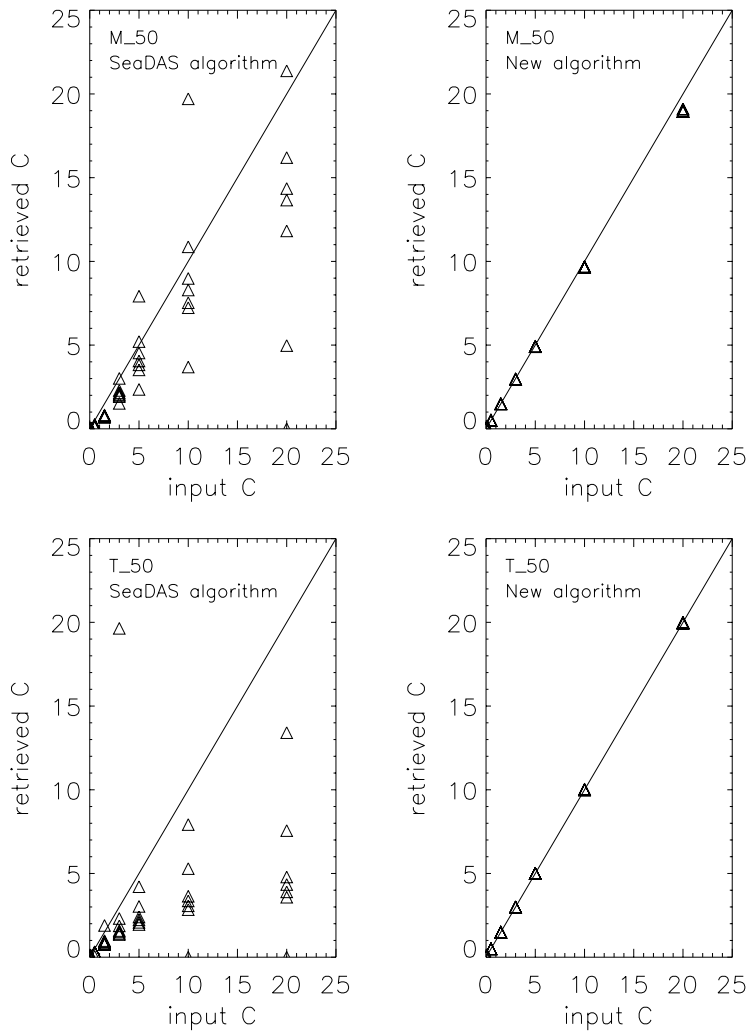

Figure 11: **Retrieved chlorophyll concentration compared to the input value. The top panels pertain to the M-50 aerosol model, and the bottom ones to the T-50 aerosol model. Left panels: SeaWiFS algorithm. Right panels: New algorithm.**

Evaluation – (5): Discussion

Figure 11 shows that:

- our new algorithm yields very accurate chlorophyll concentrations, wheras the SeaWiFS algorithm yields poor results, especially for large concentrations.

Note that:

- when τ_{865} becomes sufficiently large the SeaWiFS algorithm may overestimate the aerosol contribution to the radiance in the visible to the extent that ρ_w becomes negative: retrieval of C fails.

There are two reasons for the poor chlorophyll concentrations retrieved with the SeaWiFS algorithm:

1. 90% or more of ρ_{tot}^{meas} comes from atmosphere => ρ_w so small that: tiny error in τ_{865}^{retr} => significant error in $\rho_{path}^{TOA}(\lambda_{vis})$ => unacceptably large error in C^{retr}.
2. there are differences in the chlorophyll concentration retrieval approach between the two algorithms.

Evaluation – (6): Retrieved TOA reflectance, ρ_{path}

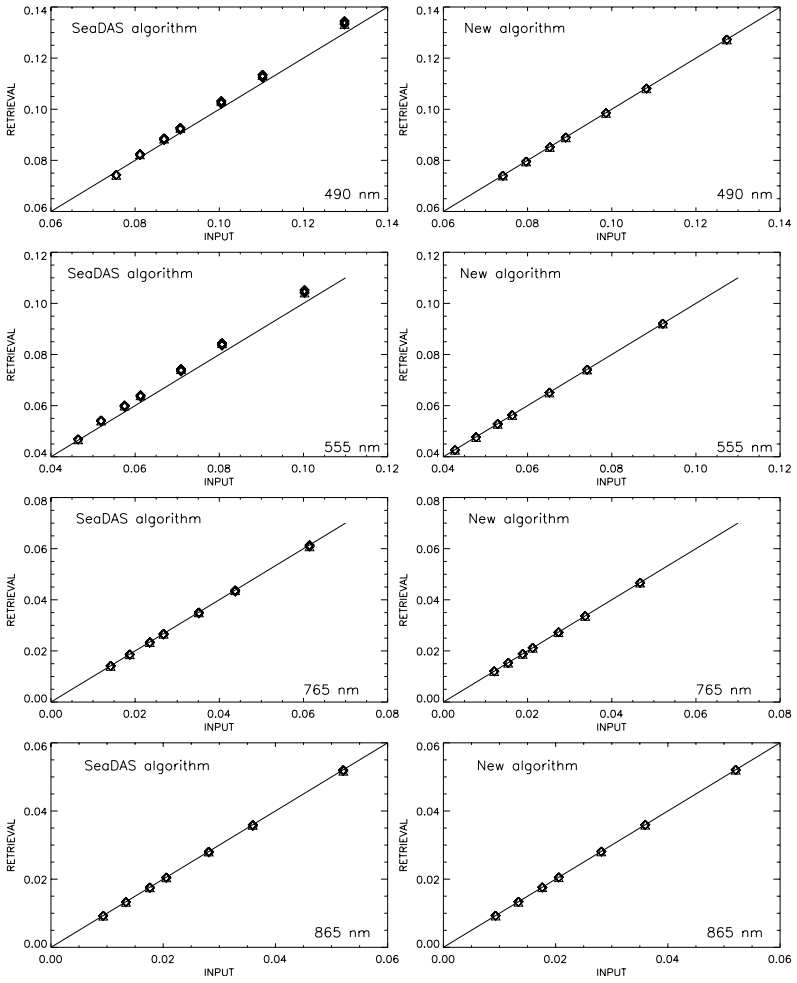

Figure 12: **Retrieved atmospheric contribution to the TOA reflectance, ρ_{path}, compared to the input value at 490, 555, 765, and 865 nm for the M-50 aerosol model. Left panels: SeaWiFS algorithm. Right panels: New algorithm.**

Evaluation – (7): Retrieved TOA water-leaving reflectance, $t\rho_w$

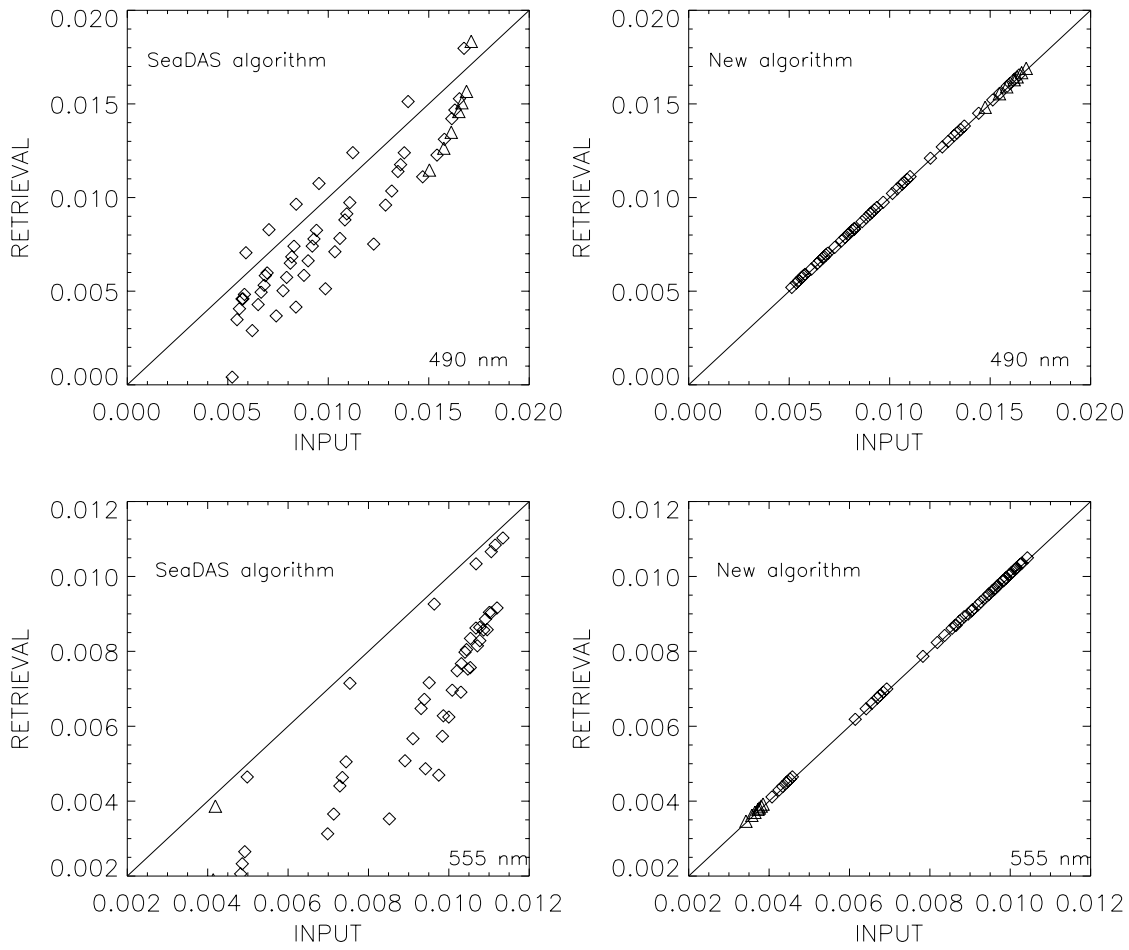

Figure 13: **Retrieved contribution of the water-leaving radiance to the TOA reflectance, $t\rho_w$, compared to the input value at 490 and 555 nm for the M-50 aerosol model. Left panels: SeaWiFS algorithm. Right panels: New algorithm.**

Evaluation – (8): Match-up data

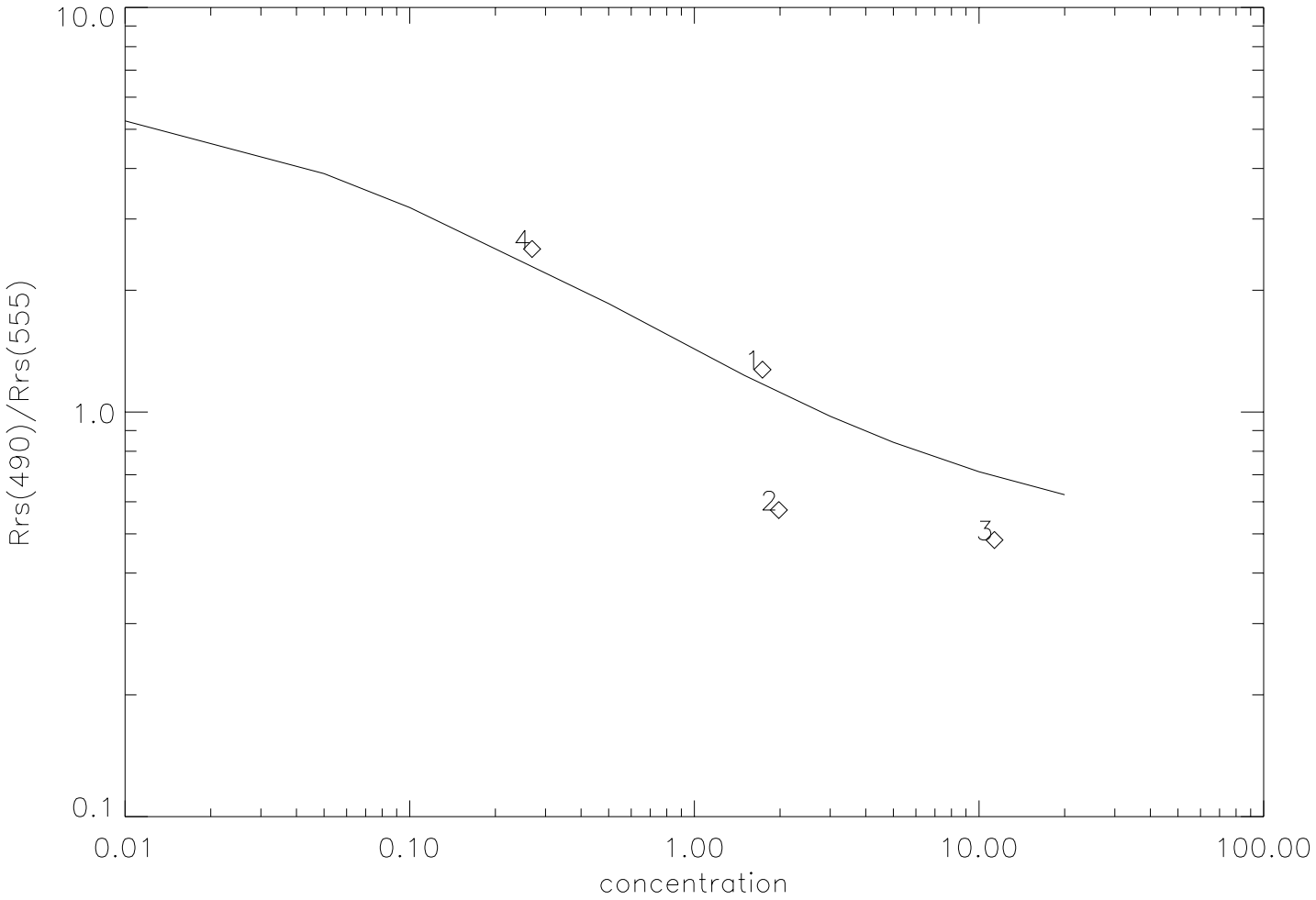

Figure 14: **$R_{rs}(490)/R_{rs}(555)$ as a function of chlorophyll concentration for the 4 match-up cases discussed in the text. The solid line represents the computed values, while the diamonds represent the field-measured values.**

Summary and Conclusions – (1)

Based on a complete IOP model and an accurate radiative transfer code for the coupled atmosphere-ocean system (CAO-DISORT), we have developed:

- an iterative algorithm for simultaneous retrieval of aerosol optical properties and chlorophyll concentrations.

To test the performance of the algorithm we created a set of synthetic testbed data by using the forward model to:

- simulate the TOA radiances for a specific sun-satellite geometry and for several combinations of aerosol optical properties and oceanic chlorophyll concentrations.

We used this synthetic data set to demonstrate that our algorithm:

- provides self-consistent and accurate retrievals of aerosol optical properties and chlorophyll concentrations.

Light and Life STEVENS Institute of Technology Laboratory

Summary and Conclusions – (2)

We expect our new algorithm to perform better than the SeaWiFS algorithm in situations with high relative humidity, because:

- our multi-component approach to the light interaction with aerosols is more realistic than the single-component approach adopted in the SeaWiFS algorithm.

Because our approach is based on accurate simulations of the radiative transfer process including multiple scattering, and accounts for the coupling between the atmosphere and the ocean:

- many of the assumptions invoked in the current SeaWiFS algorithm are avoided. Hence, it is expected to be useful for:
- addressing retrieval problems associated with absorbing aerosols as well as Case II waters (Frette et al., 1998, 2001).
- It lends itself readily to the inclusion of more complete IOP models, such as that presented by Stramski et al. (2001).

References

D. Antoine and A. Morel, (1999), A multiple scattering algorithm for atmospheric correction of remotely sensed ocean color (MERIS instrument): principle and implementation for atmospheres carrying various aerosols including absorbing ones. *Int. J. Remote Sens.*, 20, 1875-1916.

O. Frette, J. J. Stamnes, and K. Stamnes, (1998), Optical remote sensing of marine constituents in coastal waters: A feasibility study, Applied Optics, 37, 8218-8326.

O. Frette, S. R. Erga, J. J. Stamnes, and K. Stamnes, (2001), Optical remote sensing of waters with vertical structure, Applied Optics, 40, 1478-1487.

K. I. Gjerstad, (2001), Monte Carlo simulations of radiative transport in the atmopshere and ocean, M. Sc. thesis, University of Bergen.

H. R. Gordon, (1996), MODIS Normalized water-leaving radiance algorithm theoretical basis document (MOD18).

H. R. Gordon, (1997), Atmospheric correction of ocean color imagery in the Earth Observing System era. *J. Geophys. Res.*, 102 (17), 17,081-17,106.

H. R. Gordon and M. Wang, (1994), Retrieval of water-leaving radiance and aerosol optical thickness over the oceans with SeaWiFS: A preliminary algorithm. *Appl. Opt.*, 33,443-452.

Z. Jin, and K. Stamnes, (1994), Radiative transfer in nonuniformly refracting media: atmosphere-ocean system. *Appl. Opt.*, 33, 431-442.

W. Li, and K. Stamnes, (2001), Inherent optical properties of case I waters: A complete model suitable for use in radiative transfer computations. Submitted to *J. Geophys. Res.*.

A. Morel, and S. Maritorena, (2001), Bio-optical properties of oceanic waters: A reappraisal, *J. Geophys. Res.*, *106*, 7163–7180.

J. E. O'Reilly, S. Maritorena, B. G. Mitchell, D. A. Siegel, K. L. Carder, S. A. Garver, M. Kahru, and C. McClain, (1998), Ocean color chlorophyll algorithm for SeaWiFS, *J. Geophys. Res.*, *103* (C11), 24,937–24,953.

T. L. Petzold, (1972), Volume scattering functions for selected ocean waters. Scripps Inst. Oceanogr. Visibility Lab., ref. 72-78.

R. M. Pope, and E. S. Fry, (1997), Absorption spectrum (380-700nm) of pure water, II, Integrating cavity measurements, *Appl. opt.*, *36*, 8710–8723.

R. A. Reynolds, D. Stramski, and B. G. Mitchell, (2001), A chlorophyll-dependent semianalytical reflectance model derived from field measurements of absorption and backscattering coefficients within the Southern Ocean, *J. Geophys. Res.*, 106, 7125-7138.

D. A. Siegel, M. Wang, S. Maritorena, and W. Robinson, (2000), Atmospheric correction of satellite ocean color imagery: the black pixel assumption, *Appl. Opt.*, 39, 3582-3591.

R. C. Smith, and K. S. Baker, (1981), Optical properties of the clearest natural waters, *Appl. Opt.*, *20*, 177–184.

K. Stamnes, S.-C. Tsay, W. J. Wiscombe, K. and Jayaweera, (1988), Numerically stable algorithm for discrete-ordinate-method radiative transfer in mutiple scattering and emitting layered media, *Appl. Opt.*, *27*, 2502–2509.

D. Stramski, A. Bricaud, and A. Morel, (2001), Modeling the inherent optical properties of the ocean based on the detailed composition of the planktonic community, *Appl. Opt.*, 40, 2929–2945.

G. E. Thomas, and K. Stamnes, (1999), Radiative Transfer in the Atmosphere and Ocean, *(Cambridge University Press)*.

B. Yan, (2001), Radiative transfer modeling in the coupled atmosphere-ocean system and its application to the remote sensing of ocean imagery, Ph.D. dissertation, University of Alaska Fairbanks.

Yan, B., K. Stamnes, W. Li, B. Chen, J. J. Stamnes, and S. C. Tsay, (2002), Pitfalls in atmospheric correction of ocean color imagery: How should aerosol optical properties be computed?, Applied Optics, 41, 412-423.

B. Yan, and K. Stamnes, (2002), Fast yet accurate computation of the complete radiance distribution in the atmosphere-ocean system, *J. Quant Spctrosc. Radiat. Transfer*, submitted.